Microstructural Inhomogeneity in Constrained Groove Pressed Cu-Zn Alloy Sheet

Prabhat Chand Yadav, Arush Sinhal, Sandeep Sahu, Abir Roy, and Shashank Shekhar

Severe plastic deformation (SPD) is routinely employed to modify microstructure to obtain improved mechanical properties, particularly strength. Constrained groove pressing (CGP) is one of the SPD techniques that has gained prominence recently. However, the efficacy of the method in terms of homogeneity of microstructure and properties has not been well explored. In this work, we examine the microstructure and mechanical properties of CGP processed Cu-Zn alloy sheet and also explore homogeneity in their characteristics. We found that CGP is very effective in improving the mechanical properties of the alloy. Although the reduction in grain size with the number of passes in CGP is not as huge ($\sim$38 μm in annealed sample to $\sim$10.2 μm in 1 pass sample) as is expected from a SPD technique, but there is a drastic improvement in ultimate tensile strength ($\sim$230 to $\sim$380 MPa) which shows the effectiveness of this process. However, when mechanical properties were examined at smaller length scale using micro-indentation technique, it was found that hardness values of CGP processed samples were non-uniform along transverse direction with a distinct sinusoidal variation. Uniaxial tensile test data also showed strong anisotropy along principal directions. The cause of this anisotropy and non-uniformity in mechanical properties was found to lie in microstructural inhomogeneity which was found to exist at the length scale of the grooves of the die.

1. Introduction

Nanostructured materials or ultrafine-grained (UFG) materials have improved mechanical properties like hardness and strength, which make them desirable for applications requiring high specific strength. These fine-grained materials are produced from bulk materials by severe plastic deformation (SPD) technique. There are various techniques that can impose SPD to produce fine-grained microstructure. These techniques include constrained groove pressing (CGP) (Ref 1, 2), accumulated roll bonding (ARB) (Ref 3, 4), equal channel angular pressing (ECAP)/extrusion (Ref 5, 6), high-pressure torsion (HPT) (Ref 7, 8), cyclic extrusion compression (Ref 9, 10), twist extrusion (Ref 11, 12). CGP is a technique that is applied on sheet metals and plates and hence has good potential for commercial applications, while the same cannot be said for most of the other SPD techniques. CGP allows us to, theoretically, introduce uniform and large cumulative equivalent strain to the materials. It does so through repetitive shear deformation by using alternate pressing with an asymmetrical grooved and flat

die while maintaining a gap between the lower and upper die equal to the thickness of the sample. This helps to maintain only pure shear deformation under plane strain deformation conditions (Ref 13). Using this method, a uniform cumulative strain of 0-3.48 is imparted to samples in 3 CGP passes (each CGP pass imposes strain of magnitude 1.16 to the Cu-Zn alloy sheets to produce high-strength nanostructured materials) (Ref 14). Study of uniformity in microstructure and properties of materials processed using a given method, is important to establish its commercial feasibility. Several SPD techniques are known to impart non-uniform deformation and hence, microstructural inhomogeneity is inherent in such processes. Inhomogeneity along radial direction is well known in HPT and has been studied by several researchers (Ref 15, 16). Edalati et al. have shown small inhomogeneity along angular direction (Ref 15). They have also shown that this inhomogeneity reduces with increasing number of revolution of HPT. Homogeneity study on HPT of Cu-Zr alloy was also conducted by Wongsa-Ngam et al. who found large difference in hardness between edge and center of the disk for smaller number of turns (Ref 16). However, they also found that this inhomogeneity quickly disappears with increasing number of turns and homogeneous properties were obtained at higher number of turns of HPT. Wongsa-Ngam et al. also found that uniform hardness were accompanied with homogeneity in microstructure (Ref 16). Inhomogeneity studies have also been carried out in another SPD technique, viz. ECAP (Ref 17, 18). Wei et al. studied the influence of the die geometry like outer angle and the effect of external factors like friction conditions, on the inhomogeneity in mechanical properties (Ref 19). One of the important findings of their study was that the inhomogeneity in ECAP is inherent in the die geometry. Their experimental findings were consistent with their finite element method (FEM) simulation (Ref 19). FEM analysis by other researchers has also shown that significant strain inhomogeneity exists across the billet width (Ref 17). However, ECAP study of

Prabhat Chand Yadav, Arush Sinhal, Sandeep Sahu, and **Shashank Shekhar**, Department of Materials Science and Engineering, Indian Institute of Technology Kanpur, FB411, Kanpur, Uttar Pradesh 208016, India; and **Abir Roy**, Department of Applied Mechanics, Motial Nehru National Institute of Technology Allahabad, Allahabad 211004, India. Contact e-mails: yadav@iitk.ac.in, arush.sinhal@postgrad.manchester.ac.uk, ssandy@iitk.ac.in, ram1505@mnnit.ac.in, and shashank@iitk.ac.in.

eutectic Zn-5%Al alloy by G. Purcek et al. found that in certain cases ECAP can lead to improvement in homogeneity, but some inhomogeneity remains across the cross section of the sample (Ref 20). Zhu et al. also observed drop in inhomogeneity with increasing number of ECAP pass (Ref 21).

Most of these studies clearly show the existence of inherent inhomogeneity in SPD technique and hence, it results in non-homogeneous microstructure and non-uniformity in mechanical properties. However, CGP has been theoretically shown to lead to homogenous strain, and hence should be expected to result in homogenous microstructure and uniform mechanical properties (Ref 22-26). Various results are, however, in contradiction to this expectation (Ref 27, 28). Moreover, CGP process is asymmetric at the macro-level owing to the presence of grooves along one direction, and not in the perpendicular direction. It is also important to establish whether the length scale of groove can have any influence on the microstructural variation.

Ghazni and Vajd's work (Ref 29) on FEM simulation of CGP process showed that during each CGP cycle, the first grooving and flatting steps increase the strain inhomogeneity which were found to recover during second grooving and flattening steps. However, each CGP cycle showed to result in some inhomogeneous strain left at the material and never found to reach the theoretically uniform strain. Qian's group (Ref 30-32) also did FEM simulation of CGP process and showed that strain inhomogeneity exist along the width and depth direction. However, they did not study microstructural variation across the width of the strip of CGP processed sample, where they reported largest amount of strain inhomogeneity. Their model also has some lacunae as the model assumes stretching along sharp edges of the deformed sample which would not be possible without the presence of curvature along the corners (Ref 30, 33). The above-mentioned literature survey clearly demonstrates the absence of microscopic uniformity during CGP processes, however, a systematic study which could correlate the inhomogeneity in microstructure to its properties, is still lacking. Some homogeneity studies have also been conducted on CGP of pure Cu by Zhu et al. (Ref 21). Their results distinctly showed the presence of not only inhomogeneity, but also periodicity in the properties. However, the authors did not try to relate these periodic fluctuations with the microstructure of the sample.

The broad goal of this study is to study if there is any inherent inhomogeneity in the CGP process. With this aim, we study the mechanical properties of the samples after 1 pass and relate it with the microstructure. Our results indicate that inhomogeneity does indeed exist in samples processed through this technique. We show that this strain inhomogeneity can be explained using bending strains which implies that this inhomogeneity is inherent in the system. This, in turn, explains the non-uniformity in microstructure and the existence of inhomogeneity of mechanical properties at micro- and macro-level. It is likely that this inhomogeneity will diminish with increasing number of passes, however, we have limited our study to just one pass, as the focus of this study was to ascertain if inhomogeneity is inherent in the process.

2. Materials

In the present study, Cu-Zn alloy was used to study the effect of strain on mechanical properties at room temperature. The chemical composition of the alloy obtained using optical emission spectroscopy (OES) is given in Table 1.

D2 die steel was used to make CGP die for grooving and flattening of Cu-Zn alloy sheet. The sequence of grooving and flattening steps is shown in Fig. 1.

3. Experimental Procedure

In the current study, an asymmetrical die with the groove angle (θ) of 45° and groove width 1.5 mm was used, as shown in Fig. 1. A single pass (2 grooving and 2 flattening steps) of the die results in an effective equivalent strain of 1.16 throughout the sheet. Samples with the dimension of $60 \times 50 \times 1.5$ mm^3 were cut from Cu-Zn alloy sheet for CGP processing. Samples for CGP were prepared by annealing the as-received sheets at 750°C for 3 h followed by water quenching, to obtain a homogenous equiaxed microstructure. Samples were then deformed using the CGP technique up to 3 passes on a 1000 kN hydraulic press operating at a constant press speed of 0.1 mm/s at room temperature. One pass of CGP process includes 4 steps of die pressing, viz. grooving followed by flattening, rotating the sample by 180° along the axis of the plane of the sheet, and then repeating grooving and flattening steps. These steps are explained schematically in Fig. 1 (adapted from Lee et al. (Ref 34). As illustrated in the figure, one grooving process yields a strain of 0.58 in alternate strips which increases to 1.16 after that flattening process. When this process was repeated after rotating the sample, the other set of alternating strips were deformed to the strain of 1.16, thereby providing a theoretically uniform strain of 1.16 across the sheet. Similar steps were repeated for second and third pass of CGP process yielding a theoretical equivalent plastic strain of 2.32 and 3.48, respectively, across the sheet. Teflon tape was wrapped around the samples during pressing to provide necessary lubrication. CGP processed samples were polished by emery papers up to 2000 grade followed by cloth polishing using alumina powder (particle size 1.0 and 0.05 μm) for microhardness testing and electron back scattered diffraction (EBSD) characterization. For orientation imaging microscopy (OIM) characterization, additional polishing of CGP processed samples was done using electro-polishing technique with an electrolyte containing 25% H_3PO_4, 50% deionized water, and 25% Ethanol. EBSD-based OIM technique was used to characterize and quantify microstructure and grain boundaries evolved during CGP process. EBSD was done using Oxford instruments 'Nordlys' detector attached to 'Zeiss EVO50' scanning electron microscope and the data were analyzed using HKL channel 5 Tango software. EBSD scan length was chosen as 3000 μm along width (transverse direction) and 200 μm along height (longitudinal direction) with a step size of

Table 1 Composition of Cu-Zn alloy used for CGP process

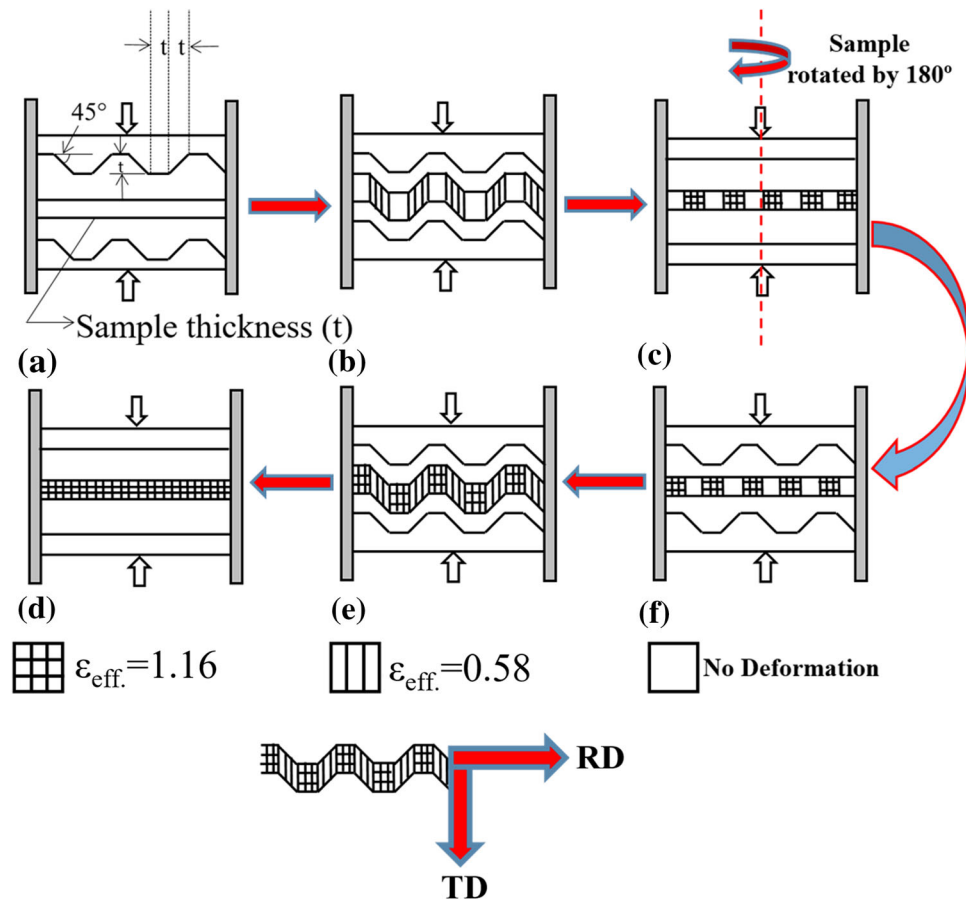| Element	Cu	Zn	Fe	C	Sn	Si	Pb	Ag	Al	S
Weight %	95.2	4.64	0.0475	0.0261	0.0295	0.0220	0.0163	0.0034	0.0028	0.0028

Fig. 1 Sequence of steps used in one pass for the CGP process (adapted from Ref 34)

1 μm. Along with microstructural characterization, mechanical properties were also tested. In order to measure change in hardness with increasing number of pass, microhardness tests were conducted on CGP processed samples using 50 g weight and 10 s dwell time. For each sample, at least 15 readings were taken on the mid-plane of the sheets. A systematic hardness test was also conducted for 1-pass sample, to study the variation in properties at smaller length scale, the details of which are given in later section. Along with hardness tests, tensile tests of CGP processed samples were also performed to evaluate the strength and ductility of the processed samples. Dog bone samples with a gauge length of 25 mm and gauge width of 6 mm (ASTM E8 M standard) were tested on a 50 kN universal testing machine (UTM) at strain rate of 6.7×10^{-4}/s.

4. Results

4.1 Microstructure

The OIM micrographs of annealed (called as '0 pass' in this manuscript) as well as CGP processed samples from 1 pass to 3 pass are shown in Fig. 2. From Fig. 2(a), it is clear that 0 pass sample has approximately equiaxed grains, but Fig. 2(b)-(d) show evidence of reduced grain size in CGP processed samples w.r.t. 0 pass. OIM images indicate that there are clusters of refined grains as well as relatively larger grains, giving it a non-homogenous character. This non-uniformity can be expected to

manifest in the properties as well. This will be discussed in more detail in the later section.

Grain size distribution from 0 pass to 3 pass CGP processed samples were also examined and is illustrated in Fig. 3. It is clear from Fig. 3 that fraction of small-sized grains increases with increasing CGP pass. Fraction of small-sized grains (grain size ≤ 10 μm) for 3 pass (largest strain) sample is approximately double than that of 0 pass (zero strain) sample.

For all the CGP processed samples, misorientation plots are shown in Fig. 4. Undeformed samples have higher fraction of high-angle grain boundaries (HAGB), as shown in Fig. 4(a). But in CGP processed samples, the grain boundary angle misorientation is largely in the range of 2°-5° as shown in Fig. 4(b)-(d). An important observation from Fig. 4 is that 1 pass, 2 pass, and 3 pass samples have larger fractions of low-angle grain boundaries (LAGBs), whereas the 0 pass sample has very small fraction of LAGBs. This is due to imposition of strains in CGP deformed samples. Deformation causes dislocations to rearrange themselves resulting in higher fraction of LAGBs.

4.2 Mechanical Properties

4.2.1 Hardness. Average hardness (VHN) along with standard deviation was calculated and is plotted with the number of CGP passes, shown in Fig. 5(a). The hardness values (VHN) continuously increased with number of passes. 0 pass sample has an average hardness of 60 VHN, which increases up to 120 VHN for 1 pass, 125 VHN for 2 pass, and
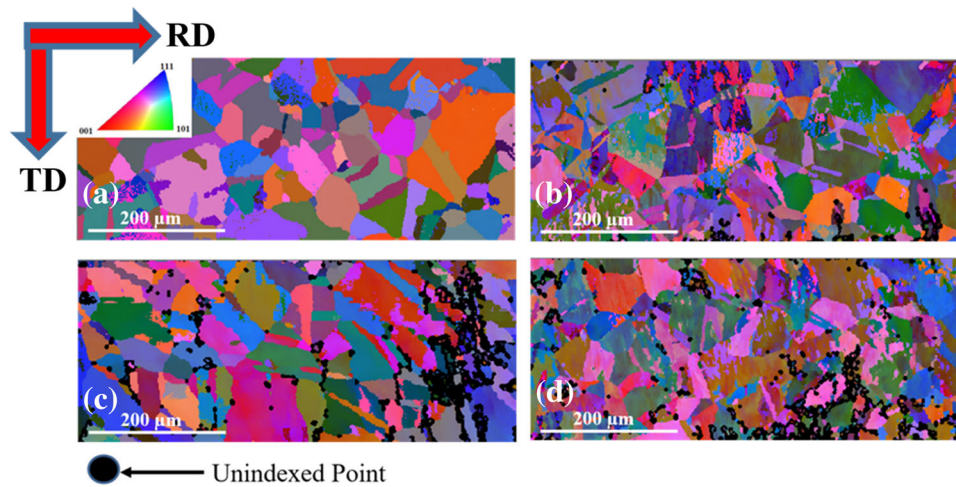
Fig. 2 EBSD Euler map of CGP sample for (a) 0 pass (b) 1 pass (c) 2 pass and (d) 3 pass showing even the smallest grains which are not visible in optical micrographs (Black points indicate un-indexed regions)
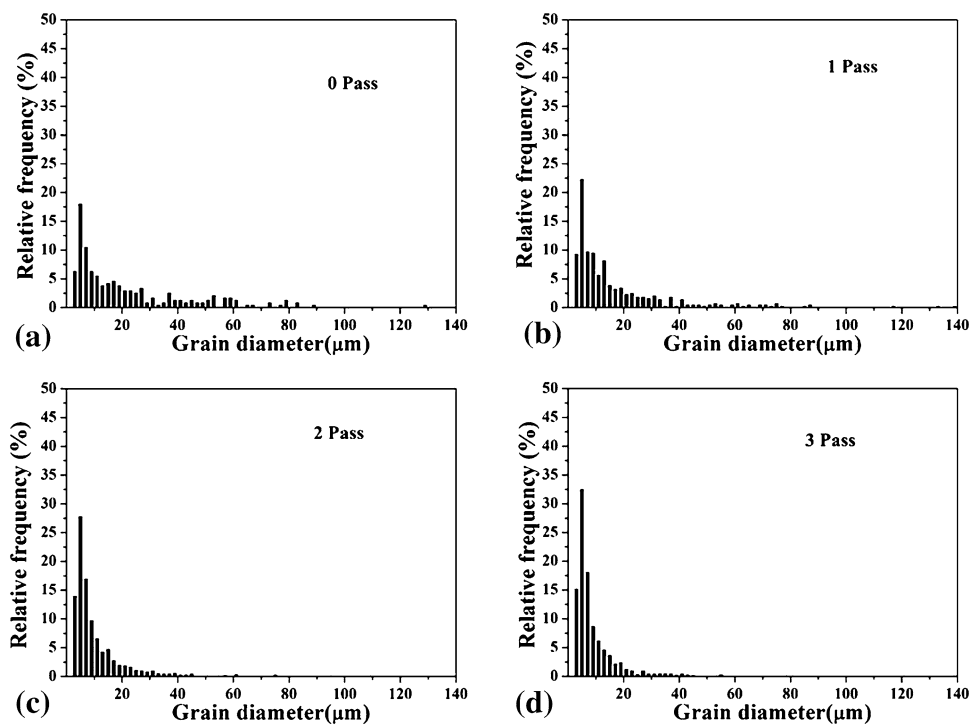

Fig. 3 Grain size distribution of CGP sample for (a) 0 pass (b) 1 pass (c) 2 pass and (d) 3 pass

130 VHN for 3 pass CGP processed sample. We obtained a significant increase in microhardness value from 0 pass to 1 pass, but the change in hardness from 1 pass onwards was not very substantial.

4.2.2 Tensile Behavior. Tensile properties of the CGP processed Cu-Zn alloy at room temperature were obtained and has been plotted in Fig. 5(b). We again observe a rapid change in mechanical behavior (in this case, increase in the yield strength (YS)) of sample from 0 pass to 1 pass. However, this trend is slightly reversed in further passes. Increase in the YS of specimens under CGP can be explained by work hardening at initial stages. High plastic deformation can occur in samples during CGP process which results in work hardening and grain

refinement. Since grain size decreases in CGP processed samples, it leads to an increase in strength of the materials according to the Hall-Petch relationship (Ref 35). In further passes, we have observed a slight decrease in YS. This can be attributed to two reasons. One is, saturation of dislocations at higher values of accumulated strain in the bulk material. At this stage, grains contain a large number of dislocations and it is not possible to produce new dislocation in these grains, however, additional strain may lead to some amount of recovery. Hence, the loss of strength in subsequent passes may be due to softening associated with recovery where dislocations rearrange in low-energy structures (Ref 36). The second cause is, microcracks that initiate on the surface of specimens which
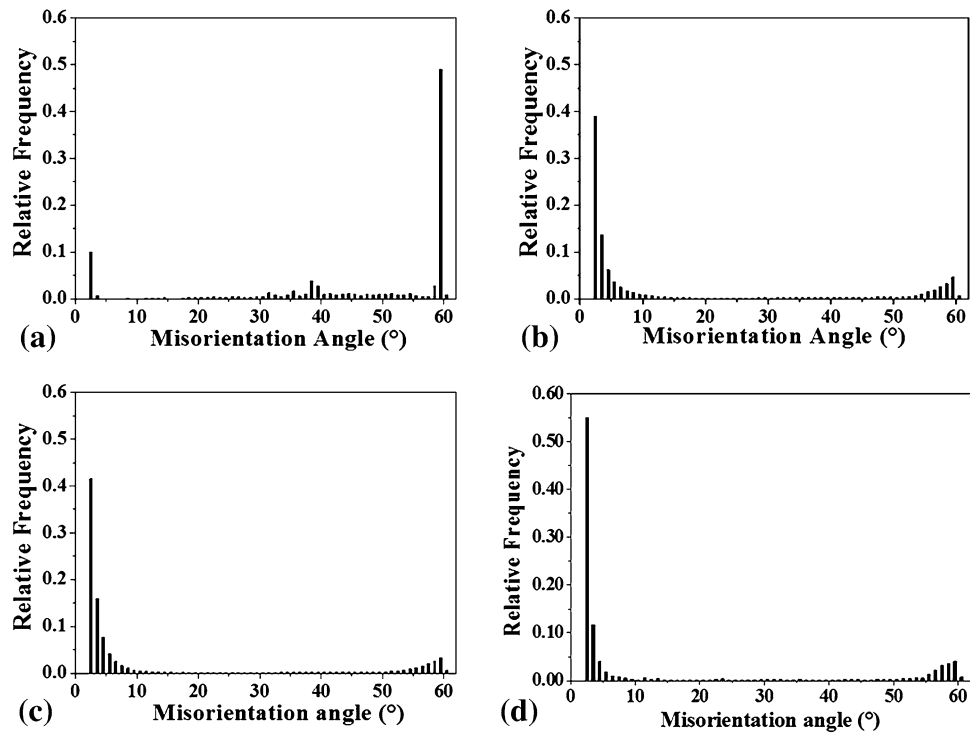
Fig. 4 EBSD misorientation plots showing the effect of mechanical processing (CGP) on misorientation angle distribution of (a) 0 pass (b) 1 pass (c) 2 pass and (d) 3 pass samples
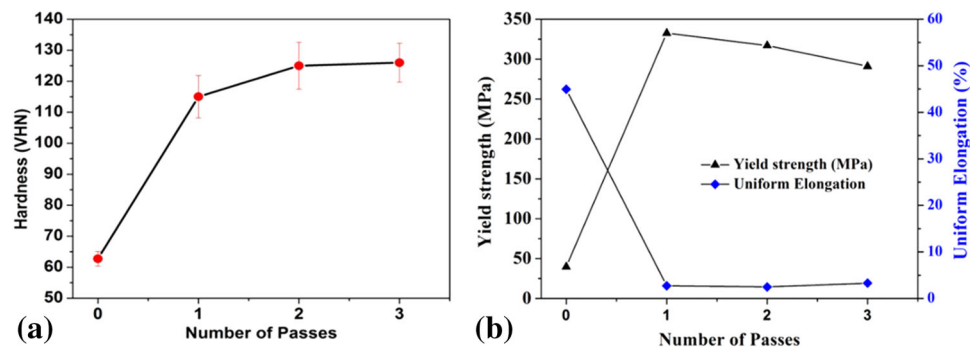

Fig. 5 Variation of (a) Vickers hardness (VHN) with standard error w.r.t. number of passes (b) tensile behavior of Cu-Zn alloy sheet with number of passes along longitudinal direction of the CGP processed sample

result in easier deformation of the material at relatively lower stresses. This can be expected especially at higher passes due to the friction and stress concentration on the corner of grooves. The trend observed for YS is similar to that obtained by other researchers (Ref 11, 37-39). As reported in Fig. 5(b), uniform elongation decreases with increasing number of passes. Uniform elongation of 0 pass samples decreases from 47 to 4% after 3 pass. Decrease in elongation in CGP processed samples can also be explained in terms of work hardening (Ref 40).

5. Analysis

The above results show that after even one pass, strength increased substantially, however, the grain refinement that accompanied it was not as high as expected from literature (Ref 13, 41-43). There are only two ways to explain this anomaly. One that even this small grain refinement ($\sim$46 to $\sim$24 μm) is sufficient to improve the strength by a large magnitude (45 to 340 MPa) that we observe. However, we know from literature that grain sizes of the order of $\sim$24 μm cannot lead to such a drastic change in strength, and hence this possibility can be ruled out (Ref 13, 42-44). The only other possibility is that the microstructure consists of both large grains and small grains where the small grains are actually contributing to the increase in strength and drop in ductility. OIM micrographs shown in Fig. 2 reinforces this understanding that clusters of small grains exist in otherwise moderately refined microstructure. As pointed out earlier, if such non-uniformity exists in microstructure, it must have origin in the CGP process and should manifest in non-uniformity or anisotropy in properties, as well.

In order to test the above hypothesis, mechanical properties at smaller length scale were measured to explore the presence
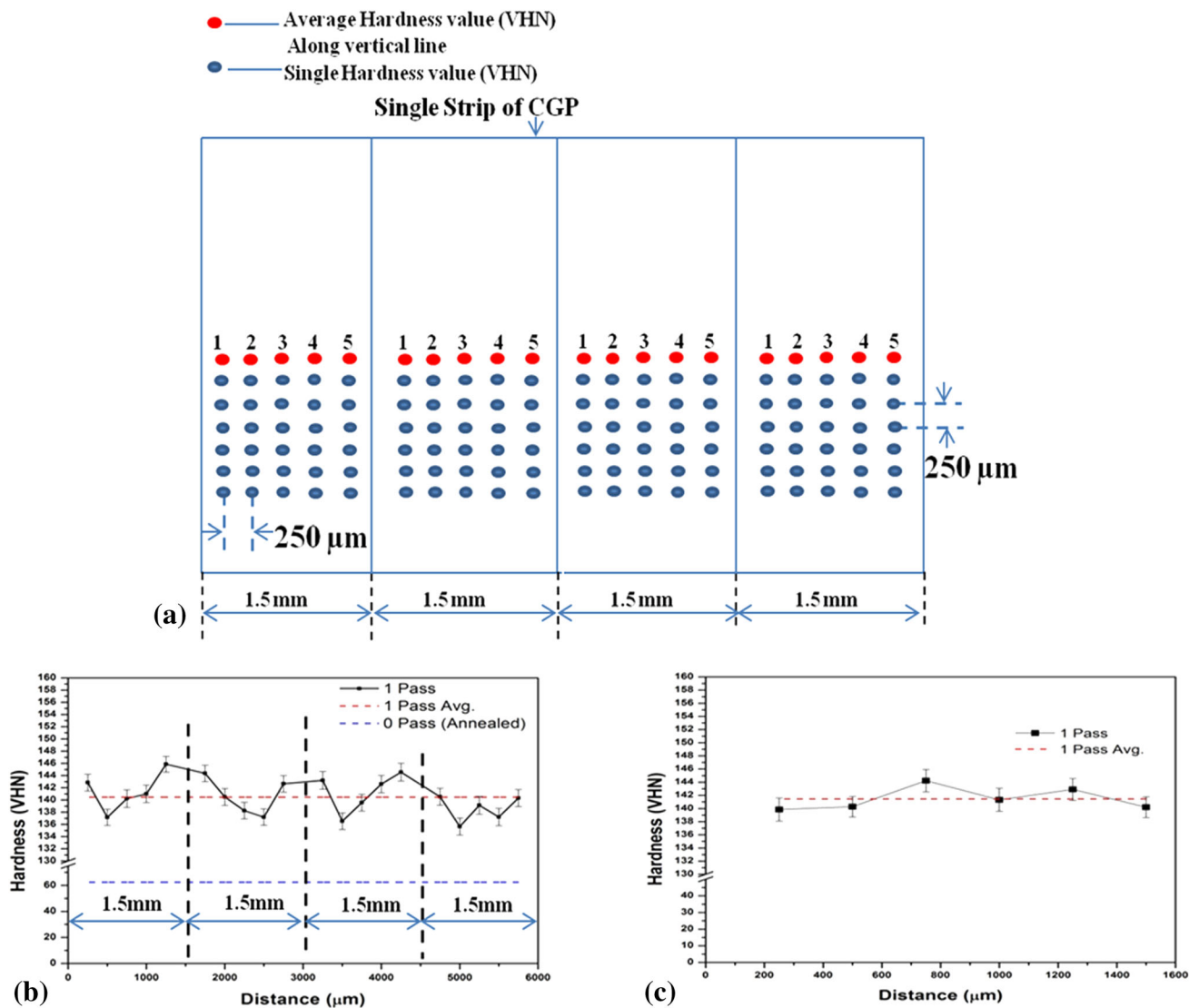
Fig. 6 (a) Schematics of hardness plot with (b) variation of microhardness (VHN) values along with standard errors w.r.t. distance along transverse direction for 1 pass CGP sample on two adjacent strips (width 6 mm) and (c) variation of microhardness (VHN) values with standard errors w.r.t. distance along longitudinal direction for 1 pass CGP sample on a single strip

Table 2   Variation of inhomogeneity factor (IF) with number of CGP passes

Longitudinal direction		Transverse direction	
Number of pass	IF	Number of pass	IF
0 pass	3.07	0 pass	3.07
1 pass	3.50	1 pass	5.47

of any inhomogeneity. Hardness test of 1 pass CGP processed sample was done using micro-indentation technique on four adjacent strips having a width of 6 mm (shown in Fig. 6) along longitudinal direction (direction of grooves) and transverse direction (perpendicular to grooves) of the CGP processed samples. The schematic of the position of indentation is shown in Fig. 6(a) where the distance between two adjacent indent points is 250 μm horizontally and vertically. The average of 6 indents was taken along direction of CGP (longitudinally) on

strip (width 6 mm) of a 1 pass CGP processed sample. Twenty such measurements (where each one is average of 6 readings along longitudinal direction of CGP direction) were taken in transverse direction. Now, the average hardness values are plotted against distance (μm) along transverse and longitudinal directions of the CGP which is shown in Fig. 6(b) and (c). We observe a "sinusoidal" variation in hardness along transverse direction, while the variation along longitudinal direction does not show such behavior. This result is the direct evidence of the
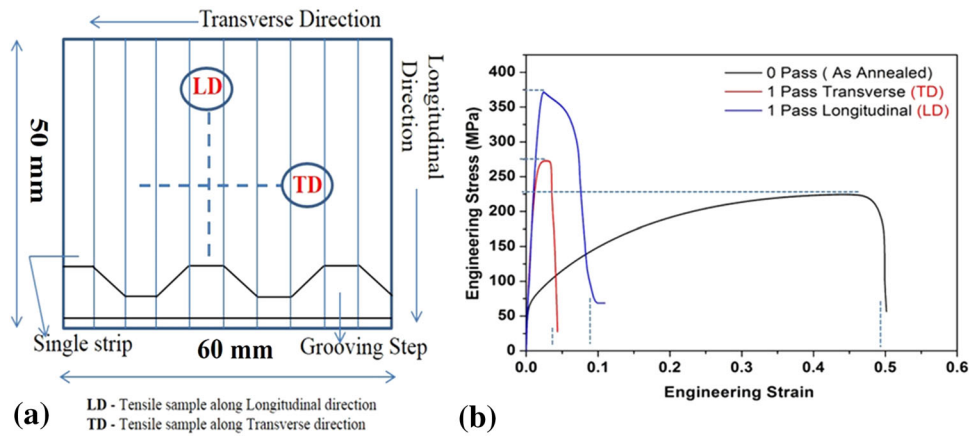
Fig. 7 (a) Schematics of tensile testing position of 0 pass and 1 pass CGP sample with (b) variation of engg. stress vs. engg. strain of 0 pass and 1 pass CGP sample
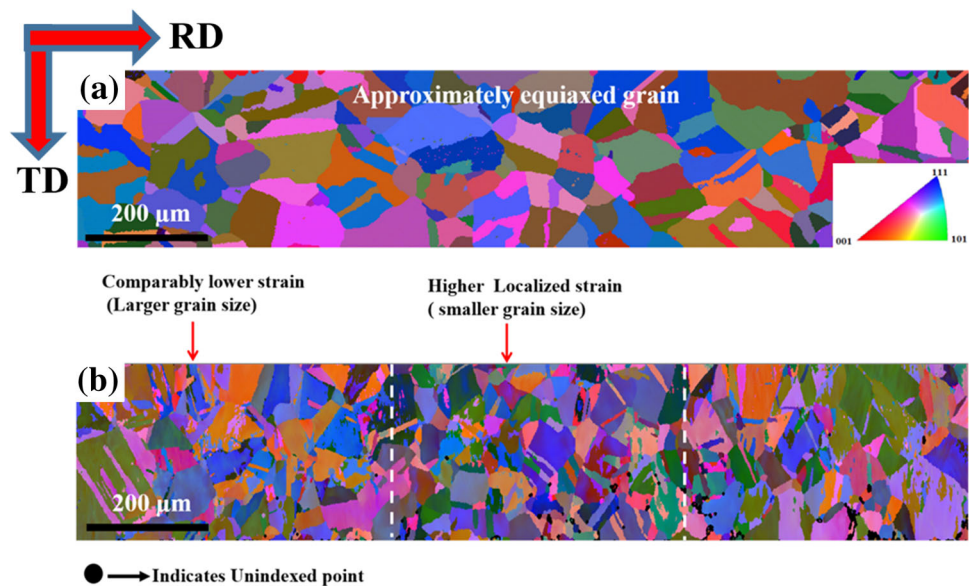

Fig. 8 Effect of equivalent strain on no. of passes on CGP processed sample shown by EBSD Euler maps for (a) 0 pass and (b) 1 pass

presence of some amount of non-uniformity in the underlying microstructure in CGP process.

5.1 Inhomogeneity Factor

In order to quantify the anisotropy observed in microhardness values in transverse and longitudinal direction, we also calculated inhomogeneity factor (IF) for 0 pass and 1 pass sample conditions (Ref 45, 46). It is given by Ref 27, 45, 46:

$$\text{IF} = \frac{\sqrt{\sum_{i=1}^{i=n}(H_i - \bar{H})^2/(n-1)}}{\bar{H}} \times 100,$$

where n is the number of hardness measurements on each sample, H_i is the hardness of ith measurement, and $\bar{H}$ is the mean hardness.

Generally, lower IF indicates higher homogeneity. IF is a meaningful parameter because it eliminates the effect of the increase of average value of sample data on the homogeneity and makes the evaluation much more reliable. This inhomogeneity in hardness values was studied along longitudinal as well as transverse direction of the CGP processed samples. Variation of inhomogeneity factor for 0 pass and 1 pass CGP processed sample is shown in Table 2 along longitudinal and transverse direction.

We clearly see that IF is approximately uniform along longitudinal direction implying that there is insignificant variation in microstructure along this direction. However, along transverse direction, there is significant variation in IF where the value of IF increases almost twofold, when we move from 0 pass to 1 pass. This large increase in IF confirms the presence of inhomogeneity in properties and microstructure along the transverse direction. As discussed earlier, this local inhomogeneity in microstructure must have origin in the fact that the region joining two grooved strips undergoes much larger
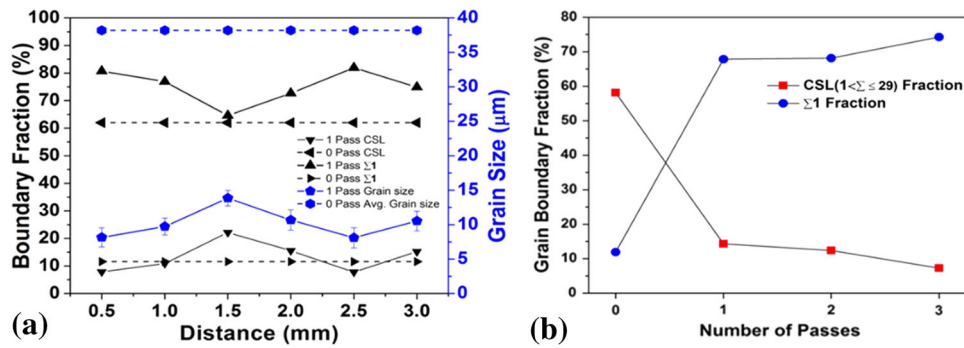
Fig. 9 (a) Variation of fraction of CSL boundary and $\Sigma 1$ boundary along transverse direction for 0 pass and 1 pass CGP processed sample. Also showing the variation of grain size with distance for 0 pass and 1 pass CGP processed samples (b) Variation of CSL boundary fraction and $\Sigma 1$ boundary fraction w.r.t. number of passes of CGP processed samples
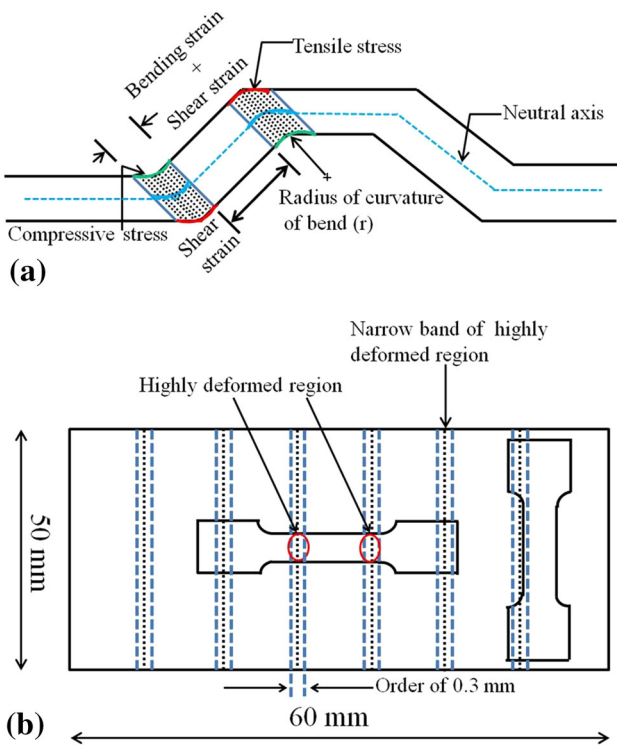

Fig. 10 Schematics of (a) different deformation zone on CGP strip and (b) position of tensile specimen along longitudinal as well as transverse direction of CGP processed sample

strains. The higher strains must lead to larger grain refinement in a narrow region around the intersection which leads to high hardness values in this narrow region.

The above hardness measurements and the IF factors have just showed inhomogeneity at smaller length scale, however, it is imperative to study whether this inhomogeneity or anisotropy exists at larger length scale. Hence, uniaxial tensile tests were also conducted for 1 pass CGP processed samples along longitudinal as well as transverse direction. The stress-strain plot for CGP processed samples is shown in Fig. 7(a) and (b).

We observe from the plot that yield strength has increased by several folds in both longitudinal and transverse direction, however, the increase in yield strength in the longitudinal direction is substantially more than that in transverse direction.

Ductility in the two directions also shows anisotropy, with it being much larger in longitudinal direction than in transverse direction. Although the overall grain size distribution is same for both the direction, a large difference is observed in the macroscopic properties. This large anisotropy can only be explained in terms of the microstructural inhomogeneity at the length scale of the grooves. As explained earlier, the region near the intersection of two grooves is exposed to larger strain and hence larger grain refinement took place and also the dislocation density is saturated in these regions. The tensile samples along the transverse direction would have alternating layers of highly refined grains and moderately refined grains. The highly refined grain, because of saturation of dislocations, can be expected to have very little or no work hardening and one of these 'weak zones' would fail quickly when put under tensile load. While the tensile sample in the longitudinal direction would also have refined grain regions, these regions would not be perpendicular to the direction of applied load and hence they will not act as "weak zones." These results indicate that microstructural inhomogeneity exists which leads to anisotropy in properties. In order to further test the hypothesis about the existence of non-uniform microstructure, we carried out EBSD-based OIM.

5.2 Electron Back Scattered Diffraction (EBSD) analysis

Grain orientation map for 0 pass and 1 pass CGP processed sample is shown in Fig. 8. In order to analyze the variation of microstructure across the grooves, grain orientation map was obtained for 1 full wavelength of the groove, which is 3 mm along the transverse direction. A small part of this whole region of 3 mm where large variation in microstructure was observed is presented in Fig. 8(b). On comparing the microstructure of 0 pass and 1 pass sample, large strain in the latter is obvious with the presence of many finer grains along with some un-indexed points, a clear sign of large deformation. One can also clearly see that the microstructure in the 0 pass sample is very homogenous throughout with large equiaxed grains. On the other hand, microstructure of 1 pass sample shows a drastic change from one region to another. It appears that some regions are more deformed with the presence of finer grains than other region.

In order to analyze the results in greater detail, we divided the 3 mm EBSD micrograph region into six divisions and calculated the grain size in each division independently. Variation of grain size along transverse direction for 0 pass
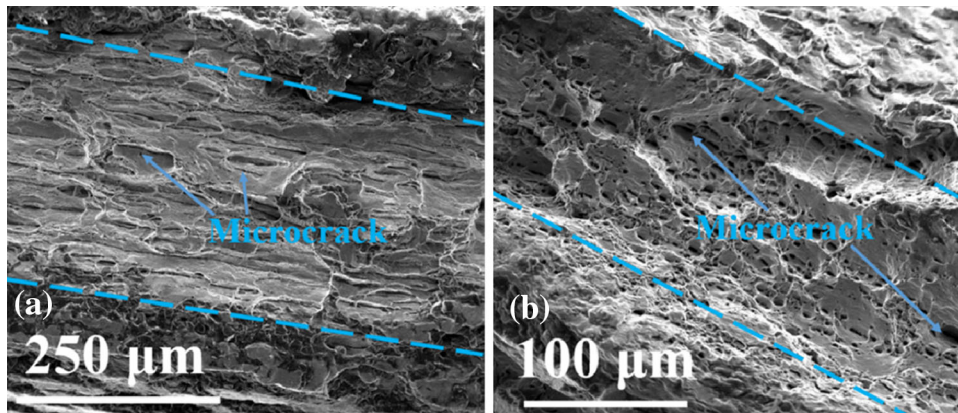
Fig. 11 SEM image of fractured surface for tensile sample along (a) transverse direction (showing brittle fracture due to several microcracks oriented perpendicular to applied stress) (b) longitudinal direction (showing ductile-like fracture along with few microcracks along applied stress)

and 1 pass is reported in Fig. 9(a). For reference, grain size for 0 pass sample (calculated from EBSD micrograph) is also shown in dotted lines (∼38 μm) in Fig. 9(a). It is clear that grain refinement has taken place for CGP processed sample and that the actual grain refinement is much higher. The more important aspect is that the grain refinement is not uniform and it actually shows some inhomogeneity along transverse direction. Average value of the grain size for 1 pass CGP processed sample was ∼10.17 μm, however, one of the divisions showed average grain size of ∼8.09 μm which is slightly smaller than the average grain size value. Moreover, the transition from small-sized grains to large-sized grains was fairly smooth, as we would expect for microstructure with continuously varying local strain. This is a very important result because it shows unambiguously that microstructural inhomogeneity exists in CGP processed sample. This microstructural inhomogeneity manifests at microscopic level in the form of local variation in microhardness values, as well as at macroscopic level, in the form of anisotropy in tensile data.

CGP is a mechanical processing technique and is also expected to transform the grain boundary character distribution. Now from EBSD data, fraction of CSL boundaries ($1 < \Sigma \leq 29$) was also calculated and plotted w.r.t. number of CGP passes. Figure 9(b) shows the variation in fraction of CSL boundary and $\Sigma 1$ boundary w.r.t. number of passes which show inverse behavior. This kind of result was also observed by Aviral et al. (Ref 47). However, drastic change is observed only between 0 pass and 1 pass CGP processed sample. Figure 9(a) shows the same boundary fraction variation w.r.t. distance along transverse direction for 1 pass. As expected, the fraction of $\Sigma 1$ boundaries increases because of increase in dislocation density which rearrange to form cell walls. Simultaneously, the CSL boundaries ($1 < \Sigma \leq 29$), which was very high for 0 pass samples, decrease to very small values even after 1 pass. However, even these boundaries show a transition across this 3 mm region, which is perhaps due to gradient in equivalent strain in the CGP processed samples along the transverse direction. This reinforces our understanding that strain inhomogeneity exists in these samples, which translates to microstructural inhomogeneity and anisotropy in mechanical properties.

5.3 Source of Strain Inhomogeneity

The results, thus far have unequivocally established that microstructural inhomogeneity exists along the transverse direction which gives rise to microstructural inhomogeneity and anisotropy in property. In this section, we present a model which explains the origin of inhomogeneity in strain for CGP processed samples.

In CGP, we ideally assume that for each half-pass (containing grooving and flattening steps), only half the region is exposed to shear strain as described in Fig. 1. This region is demarcated by a sharp bend where the metal bends and the shearing is expected to be limited up to this line of bend. However, in reality, the bend cannot be sharp and a radius of curvature is bound to develop at this corner. According to theory of bending of metals, value of strain continuously increases with decreasing radius of curvature (Ref 48, 49). So, depending on the radius of curvature that develops at the bend, a tensile and compressive strains would develop on either side of the metal sheet, as described in Fig. 10(a). During CGP process, the upper surface of sample (above the neutral axis) experiences tensile stress (shown by solid red line in Fig. 10a) and lower surface experiences compressive stress (shown by green line). After reversing the direction of sample by 180° after one set of grooving and flattening, compressive and tensile surface become interchanged. Thus, in the full cycle of CGP, the zone where two strips meet, experiences shear strain as well as bending strain, while the regions away from this intersection experience only the shear strain.

It is clear from Fig. 10(a) that CGP will lead to regions of high strains which are localized near the bends while in-between there are regions of moderate strain. The width of the high-strain region would depend on the radius of curvature of the bends. This model can easily explain the sinusoidal variation in microhardness that was observed in Fig. 6. The higher hardness corresponds to the regions which were exposed to both shear strain as well as bending strains while the regions farther away from the bends had lower hardness.

Similarly, the anisotropy in tensile test observed in Fig. 7 can also be understood using Fig. 10(b). The regions where the strains are high due to the presence of bending strain overlapping shear strain (shown by red ellipse in Fig. 10b),

formation of microcracks can be expected. Samples that were prepared along transverse direction would be expected to have microcracks perpendicular to the stress direction while those prepared along longitudinal direction would be expected to have microcracks along the stress direction. The presence of such microcracks in perpendicular direction can cause the samples to fail in a brittle manner resulting in lower yield strength and lower ductility as observed for samples prepared along transverse direction. Fractography was conducted to examine the presence of microcracks and the results are shown in Fig. 11. As pointed out in Fig. 11(a) which shows the fractograph for transverse sample, it has a large number of microcracks and that, too, in direction perpendicular to the direction of applied stress. On the other hand, the fractograph for longitudinal sample does not show such features. It does show some microcracks, but they are not present throughout the cross section and seem to be along the direction of applied stress.

6. Conclusions

After completing the constrained groove pressing process (sever plastic deformation technique) of Cu-Zn alloy sheet of 1.5 mm thickness for 0 pass, 1 pass, 2 pass, and 3 pass, by introducing theoretical equivalent plastic strain of 0, 1.16, 2.32, and 3.48, respectively, following pertinent conclusions can be drawn:

(a) Drastic increase in strength with simultaneous drop in ductility was observed in just 1 pass of CGP. The changes in strength and ductility beyond first pass were not substantial.
(b) Local inhomogeneity was observed in microhardness of 1 pass samples at the length scale of the groove of the die. The microhardness was found to have sinusoidal variation across the width of the groove. This local inhomogeneity was also found to manifest in properties at larger length scale as the tensile test showed great anisotropy in longitudinal and transverse direction.
(c) Grain size, as well as CSL boundaries, was found to be continuously varying across the width of the groove.
(d) This non-uniformity in microstructure and mechanical properties can be understood in terms of strain inhomogeneity generated due to additional bending strains near the regions where two strips meet. Hence, the observed inhomogeneity in strain is inherent in the system. This strain inhomogeneity, in turn, is responsible for non-uniformity in microstructure and the existence of inhomogeneity of mechanical properties at micro- and macrolevel.

References

1. D.H. Shin, J.-J. Park, Y.-S. Kim, and K.-T. Park, Constrained Groove Pressing and Its Application to Grain Refinement of Aluminum, *Mater. Sci. Eng. A*, 2002, **328**(1–2), p 98–103
2. F. Khodabakhshi and M. Kazeminezhad, The Effect of Constrained Groove Pressing on Grain Size, Dislocation Density and Electrical Resistivity of Low Carbon Steel, *Mater. Des.*, 2011, **32**(6), p 3280–3286
3. M. Shaarbaf and M.R. Toroghinejad, Nano-grained Copper Strip Produced by Accumulative Roll Bonding Process, *Mater. Sci. Eng. A*, 2008, **473**(1–2), p 28–33
4. S.A. Hosseini and H.D. Manesh, High-Strength, High-Conductivity Ultra-Fine Grains Commercial Pure Copper Produced by ARB Process, *Mater. Des.*, 2009, **30**(8), p 2911–2918
5. X. Molodova, G. Gottstein, M. Winning, and R.J. Hellmig, Thermal Stability of ECAP Processed Pure Copper, *Mater. Sci. Eng. A*, 2007, **460–461**, p 204–213
6. F. Al-Mufadi and F. Djavanroodi, Effect of Equal Channel Angular Pressing Process on Impact Property of Pure Copper, *Int. J. Chem. Nucl. Mater. Metall. Eng.*, 2014, **8**(1), p 30–34
7. Z. Horita and T.G. Langdon, Achieving Exceptional Superplasticity in a Bulk Aluminum Alloy Processed by High-Pressure Torsion, *Scr. Mater.*, 2008, **58**(11), p 1029–1032
8. G. Khatibi, J. Horky, B. Weiss, and M.J. Zehetbauer, High Cycle Fatigue Behaviour of Copper Deformed by High Pressure Torsion, *Int. J. Fatigue*, 2010, **32**(2), p 269–278
9. R.Z. Valiev and T.G. Langdon, Principles of Equal-Channel Angular Pressing as a Processing Tool for Grain Refinement, *Prog. Mater. Sci.*, 2006, **51**(7), p 881–981
10. A. Babaei and M.M. Mashhadi, Tubular Pure Copper Grain Refining by Tube Cyclic Extrusion-Compression (TCEC) as a Severe Plastic Deformation Technique, *Prog. Nat. Sci. Mater. Int.*, 2014, **24**(6), p 623–630
11. Y. Beygelzimer, V. Varyukhin, S. Synkov, and D. Orlov, Useful Properties of Twist Extrusion, *Mater. Sci. Eng. A*, 2009, **503**(1–2), p 14–17
12. M.I. Latypov, E.Y. Yoon, D.J. Lee, R. Kulagin, Y. Beygelzimer, and M. Seyed, Salehi, and H. S. Kim, Microstructure and Mechanical Properties of Copper Processed by Twist Extrusion with a Reduced Twist-Line Slope, *Metall. Mater. Trans. A*, 2014, **45**(4), p 2232–2241
13. A. Krishnaiah, U. Chakkingal, and P. Venugopal, Applicability of the Groove Pressing Technique for Grain Refinement in Commercial Purity Copper, *Mater. Sci. Eng. A*, 2005, **410–411**, p 337–340
14. G.G. Niranjan and U. Chakkingal, Deep Drawability of Commercial Purity Aluminum Sheets Processed by Groove Pressing, *J. Mater. Process. Technol.*, 2010, **210**(11), p 1511–1516
15. K. Edalati, T. Fujioka, and Z. Horita, Microstructure and Mechanical Properties of Pure Cu Processed by High-Pressure Torsion, *Mater. Sci. Eng. A*, 2008, **497**(1–2), p 168–173
16. J. Wongsa-Ngam, M. Kawasaki, Y. Zhao, and T.G. Langdon, Microstructural Evolution and Mechanical Properties of a Cu–Zr alloy Processed by High-Pressure Torsion, *Mater. Sci. Eng. A*, 2011, **528**(25–26), p 7715–7722
17. S. Li, M.A.M. Bourke, I.J. Beyerlein, D.J. Alexander, and B. Clausen, Finite Element Analysis of the Plastic Deformation Zone and Working Load in Equal Channel Angular Extrusion, *Mater. Sci. Eng. A*, 2004, **382**(1–2), p 217–236
18. V. Patil Basavaraj, U. Chakkingal, and T.S. Prasanna Kumar, Study of Channel Angle Influence on Material Flow and Strain Inhomogeneity in Equal Channel Angular Pressing Using 3D Finite Element Simulation, *J. Mater. Process. Technol.*, 2009, **209**(1), p 89–95
19. W. Wei, A.V. Nagasekhar, G. Chen, Y. Tick-Hon, and K.X. Wei, Origin of Inhomogenous Behavior During Equal Channel Angular Pressing, *Scr. Mater.*, 2006, **54**(11), p 1865–1869
20. G. Purcek, B.S. Altan, I. Miskioglu, and P.H. Ooi, Processing of Eutectic Zn-5% Al Alloy by Equal-Channel Angular Pressing, *J. Mater. Process. Technol.*, 2004, **148**(3), p 279–287

21. C.F. Zhu, F.P. Du, Q.Y. Jiao, X.M. Wang, A.Y. Chen, F. Liu, and D. Pan, Microstructure and Strength of Pure Cu with Large Grains Processed by Equal Channel Angular Pressing, *Mater. Des.*, 2013, **52**, p 23–29

22. Z.S. Wang, Y.J. Guan, L.B. Song, and P. Liang, *Finite Element Analysis and Deformation Homogeneity Optimization of Constrained Groove Pressing. Applied Mechanics and Materials*, Trans Tech Publications, Dürnten, 2013, p 505–513

23. K.S. Fong, D. Atsushi, T.M. Jen, and B.W. Chua, Effect of Deformation and Temperature Paths in Severe Plastic Deformation Using Groove Pressing on Microstructure, Texture, and Mechanical Properties of AZ31-O, *J. Manuf. Sci. Eng.*, 2015, **137**(5), p 051004

24. A. Shirdel, A. Khajeh, and M.M. Moshksar, Experimental and Finite Element Investigation of Semi-constrained Groove Pressing Process, *Mater. Des.*, 2010, **31**(2), p 946–950

25. A. Sajadi, M. Ebrahimi, and F. Djavanroodi, Experimental and Numerical Investigation of Al Properties Fabricated by CGP Process, *Mater. Sci. Eng. A*, 2012, **552**, p 97–103

26. Z.-S. Wang, Y.-J. Guan, G.-C. Wang, and C.-K. Zhong, Influences of Die Structure on Constrained Groove Pressing of Commercially Pure Ni Sheets, *J. Mater. Process. Technol.*, 2015, **215**, p 205–218

27. F. Khodabakhshi, M. Kazeminezhad, and A.H. Kokabi, Constrained Groove Pressing of Low Carbon Steel: Nano-structure and Mechanical Properties, *Mater. Sci. Eng. A*, 2010, **527**(16–17), p 4043–4049

28. F. Khodabakhshi, M. Abbaszadeh, H. Eskandari, and S.R. Mohebpour, Application of CGP-Cross Route Process for Microstructure Refinement and Mechanical Properties Improvement in Steel Sheets, *J. Manuf. Process.*, 2013, **15**(4), p 533–541

29. M.S. Ghazani and A. Vajd, Finite Element Analysis of the Groove Pressing of Aluminum Alloy, *Model. Simul. Mater. Sci. Eng.*, 2014, **4**(1), p 32–36

30. K. Peng, L. Su, L.L. Shaw, and K.W. Qian, Grain Refinement and Crack Prevention in Constrained Groove Pressing of Two-Phase Cu-Zn Alloys, *Scr. Mater.*, 2007, **56**(11), p 987–990

31. K. Peng, Y. Zhang, L.L. Shaw, and K.W. Qian, Microstructure Dependence of a Cu-38Zn Alloy on Processing Conditions of Constrained Groove Pressing, *Acta Mater.*, 2009, **57**(18), p 5543–5553

32. K. Peng, X. Mou, J. Zeng, L.L. Shaw, and K.W. Qian, Equivalent Strain, Microstructure and Hardness of H62 Brass Deformed by Constrained Groove Pressing, *Comput. Mater. Sci.*, 2011, **50**(4), p 1526–1532

33. X. Mou, K. Peng, J. Zeng, L.L. Shaw, and K.W. Qian, The Influence of the Equivalent Strain on the Microstructure and Hardness of H62 Brass Subjected to Multi-cycle Constrained Groove Pressing, *J. Mater. Process. Technol.*, 2011, **211**(4), p 590–596

34. J.W. Lee and J.J. Park, Numerical and Experimental Investigations of Constrained Groove Pressing and Rolling for Grain Refinement, *J. Mater. Process. Technol.*, 2002, **130–131**, p 208–213

35. F. Khakbaz and M. Kazeminezhad, Work Hardening and Mechanical Properties of Severely Deformed AA3003 by Constrained Groove Pressing, *J. Manuf. Process.*, 2012, **14**(1), p 20–25

36. F. Humphreys and M. Hatherly, *Recrystallization and Related Annealing Phenomena*, Pergamon Press, Oxford, 1995

37. M. Richert, Q. Liu, and N. Hansen, Microstructural Evolution Over a Large Strain Range in Aluminium Deformed by Cyclic-Extrusion-Compression, *Mater. Sci. Eng. A*, 1999, **260**(1–2), p 275–283

38. B. Hadzima, M. Janeček, Y. Estrin, and H.S. Kim, Microstructure and Corrosion Properties of Ultrafine-Grained Interstitial Free Steel, *Mater. Sci. Eng. A*, 2007, **462**(1–2), p 243–247

39. B. Tolaminejad and K. Dehghani, Microstructural Characterization and Mechanical Properties of Nanostructured AA1070 Aluminum After Equal Channel Angular Extrusion, *Mater. Des.*, 2012, **34**, p 285–292

40. A. Mishra, B.K. Kad, F. Gregori, and M.A. Meyers, Microstructural Evolution in Copper Subjected to Severe Plastic Deformation: Experiments and Analysis, *Acta Mater.*, 2007, **55**(1), p 13–28

41. A. Yamashita, Z. Horita, and T.G. Langdon, Improving the Mechanical Properties of Magnesium and a Magnesium Alloy Through Severe Plastic Deformation, *Mater. Sci. Eng. A*, 2001, **300**(1–2), p 142–147

42. A. Krishnaiah, U. Chakkingal, and P. Venugopal, Production of Ultrafine Grain Sizes in Aluminium Sheets by Severe Plastic Deformation Using the Technique of Groove Pressing, *Scr. Mater.*, 2005, **52**(12), p 1229–1233

43. N.D. Stepanov, A.V. Kuznetsov, G.A. Salishchev, G.I. Raab, and R.Z. Valiev, Effect of Cold Rolling on Microstructure and Mechanical Properties of Copper Subjected to ECAP with Various Numbers of Passes, *Mater. Sci. Eng. A*, 2012, **554**, p 105–115

44. M. Ebrahimi and F. Djavanroodi, Experimental and Numerical Analyses of Pure Copper During ECFE Process as a Novel Severe Plastic Deformation Method, *Prog. Nat. Sci. Mater. Int.*, 2014, **24**(1), p 68–74

45. V.Y. Gertsman and S.M. Bruemmer, Study of Grain Boundary Character Along Intergranular Stress Corrosion Crack Paths in Austenitic Alloys, *Acta Mater.*, 2001, **49**(9), p 1589–1598

46. M. Qian and J.C. Lippold, The Effect of Annealing Twin-Generated Special Grain Boundaries on HAZ Liquation Cracking of Nickel-Base Superalloys, *Acta Mater.*, 2003, **51**(12), p 3351–3361

47. A. Vaid, K. Mittal, S. Sahu, and S. Shekhar, Controlled Evolution of Coincidence Site Lattice Related Grain Boundaries, *Trans. Indian Inst. Met.*, 2016. doi:10.1007/s12666-016-0834-7

48. J. Lubahn and G. Sachs, Bending of an Ideal Plastic Metal, *Trans. ASME*, 1950, **72**, p 201–208

49. B.W. Shaffer and E.E. Ungar, Mechanics of the Sheet-Bending Process, *J. Appl. Mech.*, 1960, **27**(1), p 34–40